Depolarization effect on optical control of exciton states confined in GaAs thin films

Yamashita, Takae
Kojima, Osamu
Kita,Takashi
Isu, Toshiro

(Citation)
Journal of Applied Physics,110(4):043514-043514

(Issue Date)
2011-08-15

(Resource Type)
journal article

(Version)
Version of Record

(URL)
https://hdl.handle.net/20.500.14094/90001616

Depolarization effect on optical control of exciton states confined in GaAs thin films

Takae Yamashita,[1] Osamu Kojima,[1,a)] Takashi Kita,[1] and Toshiro Isu[2]
[1]*Department of Electrical and Electronic Engineering, Graduate School of Engineering, Kobe University, 1-1 Rokkodai, Nada, Kobe 657-8501, Japan*
[2]*Center for Frontier Research of Engineering, Institute of Technology and Science, The University of Tokushima, 2-1 Minamijosanjima-cho, Tokushima 770-8506, Japan*

(Received 14 February 2011; accepted 9 July 2011; published online 19 August 2011)

We report the effects of depolarization on the excitonic Rabi oscillation in GaAs thin films measured in the $2k_1 - k_2$ direction of a degenerate four-wave-mixing signal. The Rabi frequency, measured by changing the k_2 pulse intensity, varies with the k_1 pulse intensity; the Rabi frequency decreases with an increase in the k_1 power. This decrease originates from the reduction in the field intensity of the k_2 pulse, which consists of the local field and depolarization terms. Cancellation of the k_2 field due to depolarization leads to the decrease in the Rabi frequency. © *2011 American Institute of Physics*. [doi:10.1063/1.3624667]

I. INTRODUCTION

Various materials, such as semiconductor nanostructures, have been extensively studied with the aim of developing ultrafast information processing devices that can deal with vast amounts of data.[1,2] Although the optical nonlinear response induced by excitons in semiconductors is an attractive phenomenon with regard to these devices, the finite lifetime of this response, which is longer than input-pulse separation, results in problems in switching operations at a high repetition rate.[3] Thus, ultrafast optical control of the excitonic states by means of interaction with photons, for instance, through Rabi flopping, has been proposed.[4]

In the Rabi flopping process, the causes of deviation in the excitonic Rabi frequency and intensity damping are a subject of intense debate. Possible explanations, such as excitation of multiexciton transitions, acoustic-phonon mediated dephasing, inhomogeneity of excitation fields, and depolarization effects, have been considered. Multiexciton transitions damp the Rabi rotation because of detuning.[5] In the phonon model, coupling with lattice vibrations via the deformation potential modulates the Rabi oscillation.[6] The inhomogeneity of the excitation field in quantum dot ensembles with a large inhomogeneous width leads to damping because of the distribution of the pulse area and dipole moment.[7,8] Moreover, the external light field is split into local field and depolarization terms; the depolarization factor cancels the external fields and increases with the power of input light for the Rabi operation and for the coherent manipulation of excitonic states to operate the all-optical switches.[9–11]

We have focused on the excitonic characteristics confined in GaAs thin films with the thickness of 110 nm.[12–16] In the thin films, the long-wavelength approximation does not hold and the concept of the Rabi oscillation based on the atomic systems is strictly invalid. However, as discussed in our previous report, the excitons confined in the thin films exhibit the Rabi oscillation behavior.[13] On the other hand, the polarization Rabi oscillation, measured by a degenerate four-wave-mixing (DFWM) technique, exhibits large deviation from the Rabi frequency in a larger pulse area region; accordingly, understanding the similarity between the Rabi oscillations in weak confinement regimes and the Rabi oscillations in strong confinement regimes is important for realizing coherent control of the exciton states. In particular, coherent control of the excitons in the thin films requires revealing the depolarization effect. To our knowledge, excitonic Rabi oscillation has not been reported in such thick semiconductor systems, and hence, the effect of the depolarization factor is unclear. In this work, we present the effects of depolarization on the Rabi oscillation in the optical response of excitons confined in GaAs thin films by use of a DFWM technique. According to the k_2-power (P_{k_2}) dependence of the two-beam DFWM signal in the $2k_1 - k_2$ direction at various k_1 powers (P_{k_1}), the value of the Rabi frequency varies with P_{k_1}. We discuss the Rabi frequency change based on the depolarization effect.

II. EXPERIMENT

A sample used in the present study is a double heterostructure thin film with three periods of GaAs(110 nm)/$Al_{0.3}Ga_{0.7}As$ (5 nm) grown on a (001) GaAs substrate by molecular beam epitaxy. The enhancement of the nonlinear optical response of confined excitons in a thin film with a thickness of approximately 110 nm has been reported; this enhancement occurs due to strong coupling with the light field originating from a nonlocal response.[17] The nonlinear optical response of the excitons was measured by using a DFWM technique at 3.4 K in the backward direction of $2k_1 - k_2$. The light source was a mode-locked Ti:sapphire pulse laser with a repetition rate of 80 MHz and a pulse width Δt of 95 fs. The pulse was in the form of a sech^2 function and the spectral width was 11.4 meV, corresponding to $\Delta\nu = 2.76$ THz. This pulse was slightly different from a transform-limited pulse, since the value of the product $\Delta\nu\Delta t$ was calculated to be 0.262. The pulse train was split into two pulses, k_1 and k_2, which were both focused on a single 285-μm-diameter spot on the sample, measured with a charge-coupled-device

a)Electronic mail: kojima@phoenix.kobe-u.ac.jp.

camera. The k_1 and k_2 pulses were copolarized. According to the photon echo scheme, the k_1 (k_2) pulse corresponds to the probe (pump) pulse. The central energy was 1.5158 eV, which was the lowest exciton energy of the sample.[12,14–16] In time-domain DFWM measurements, a fast-scan system equipped with a shaker having a frequency of 20 Hz was employed instead of a conventional lock-in detection system.

III. RESULTS AND DISCUSSION

A. Rabi frequency shift

Figure 1(a) shows the dependence of the DFWM signal on P_{k_1} when P_{k_2} was kept at 0.10 mW. The DFWM signal originates from the optical nonlinearity of the confined excitons, and the ultrafast response comparable with the pulse width around zero-delay results from the overlapping of the oscillatory structures; these oscillatory structures are induced by the interference between the confined exciton states.[12] The intensity of the DFWM signal increases with P_{k_1}. In order to clarify the dependence of the DFWM intensity on P_{k_1}, the dependence of the intensity at zero-delay I_{DFWM} was plotted as a function of P_{k_1}, as shown in the inset of Fig. 1(a). I_{DFWM} is not linearly proportional to P_{k_1}. In the case of Rabi oscillation, the power dependence is described by the following equation:[18]

$$I_{\mathrm{DFWM}}(\Theta_1, \Theta_2) \propto \sin^2(\Theta_2)\sin^4(\Theta_1/2). \quad (1)$$

Here, Θ_1 (Θ_2) represents the area of the k_1 (k_2) pulse defined as $\Theta_i = pE_i\Delta t/\hbar (i = 1 \text{ or } 2)$, where p is the transition dipole moment of the exciton, E is the electric-field amplitude of the optical pulse, and $\hbar$ is Dirac's constant. Thus, Θ_i is proportional to $\sqrt{P_{k_i}}$. Although this formula is defined in the case that the temporal separation between the k_1 and k_2 pulses is larger than the pulse width, we assumed that the effects induced by the pulse width are negligible for excitons with a fast dephasing rate. We performed a fitting using a function form of $\sin^4(\sqrt{P_{k_1}}/2)$ on I_{DFWM}, as shown in Fig. 1(b). Here, we extrapolated the intensity value of zero at $P_{k_1} = 0$. The fitting result is shown by the solid curve. I_{DFWM} clearly depends on $\sin^4(\sqrt{P_{k_1}}/2)$, which indicates the Rabi oscillation of excitonic polarization.

To clarify the depolarization effect due to the exciton generated by the k_1 pulse on the Rabi oscillation generated by the k_2 pulse, we measured the P_{k_2} dependence of the DFWM signal at various P_{k_1} values. The results are shown in Fig. 2(a), which shows I_{DFWM} as a function of $\sqrt{P_{k_2}}$. The P_{k_2} dependence for each P_{k_1} was normalized by the

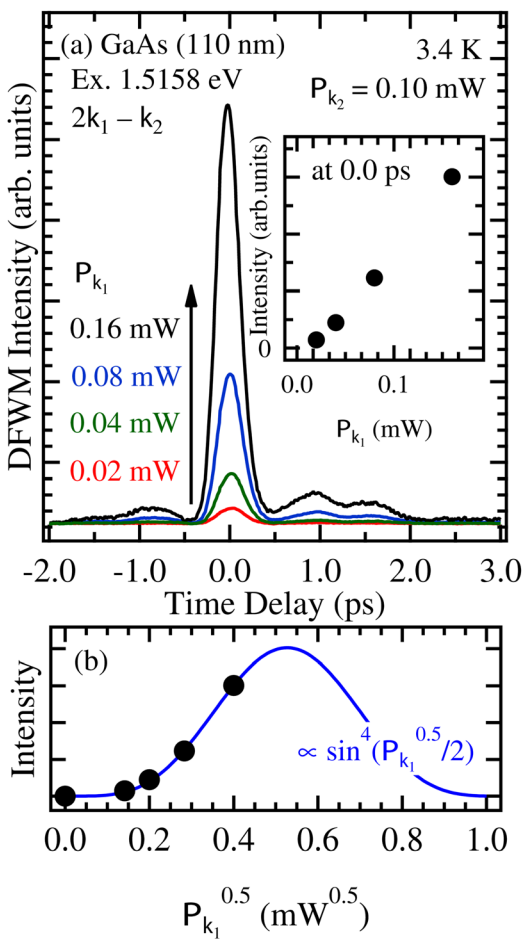

FIG. 1. (Color online) (a) DFWM signals in GaAs thin films observed at various P_{k_1} values. P_{k_2} is kept at 0.10 mW. The inset shows the P_{k_1} dependence of the signal intensity. (b) Analysis of signal intensity based on Rabi oscillation. The solid curve indicates the fitting curve.

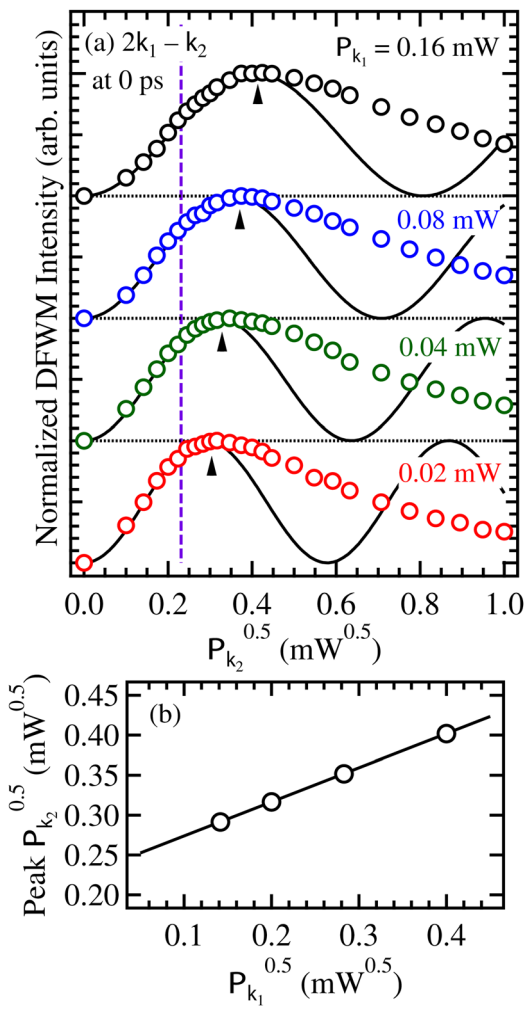

FIG. 2. (Color online) (a) P_{k_2} dependence of the DFWM signal measured at various P_{k_1} values. Solid curves indicate the analysis curves based on the Rabi oscillation. Arrows show P_{k_2} reaching a maximum intensity. (b) Peak $P_{k_2}^{0.5}$ as a function of $P_{k_1}^{0.5}$. The solid line indicates the linear fitting.

corresponding maximum intensity. As P_{k_1} increases, P_{k_2}, exhibiting the maximum intensity, also increases; meanwhile, the total exciton density increases with P_{k_1}. This result supports the concept that the decrease in signal intensity arises from the Rabi oscillation and not from high-density excitation effects. The shift to the higher P_{k_2} side of the maximum intensity, denoted by arrows in Fig. 2(a), indicates a decrease in the Rabi frequency with increasing P_{k_1}.

Based on Eq. (1), the analysis curves of the P_{k_2} dependence of I_{DFWM} are obtained; these curves are shown in Fig. 2(a) as solid curves. The peak $\sqrt{P_{k_2}}$, exhibiting the maximum I_{DFWM}, is plotted as a function of $\sqrt{P_{k_1}}$ in Fig. 2(b) (open circles). The peak $\sqrt{P_{k_2}}$ is linearly proportional to $\sqrt{P_{k_1}}$. The solid line indicates the result of least squares fitting to the experimental results. From this fitting, the $\sqrt{P_{k_1}}$ dependence of the peak $\sqrt{P_{k_2}}$ is given by $0.427\sqrt{P_{k_1}} + 0.231\ \mathrm{mW}^{0.5}$. The intercept of $\sqrt{P_0} = 0.231\ \mathrm{mW}^{0.5}$ is shown by the dashed line in Fig. 2(a). When this value of the intercept originates from the intrinsic exciton dipole moment of this sample,[19] the evaluation of p is possible using the relation $pE\Delta t/\hbar = \pi/2$. The evaluated excitonic (quasi-) dipole moment is 2000 D.

To clarify the effect of excitation-induced dephasing on the shift of the peak $\sqrt{P_{k_2}}$, we focused on the dephasing of the signal shown in Fig. 1(a). As shown in Fig. 3(a), the time-domain signals exhibit a complex oscillatory structure, due to the excitonic quantum beats,[12] and thus, evaluation of the dephasing time by fitting the temporal curves is difficult. Instead of the usual formula for the quantum beats in the DFWM signals,[20] we performed the fitting with the following simplified expression:

$$I(t) \propto C_1 \mathrm{e}^{-t/\tau_1} + C_2 \cos(\omega t + \phi)\mathrm{e}^{-t/\tau_2}, \tag{2}$$

where the first term decides the overall signal decay profile and the second term describes the oscillation-like behavior, that is, the decrease and increase in the signal intensity after 0.5 ps. In this expression, τ_1 is the overall signal decay time, τ_2 is the decay time of the oscillation-like behavior, ω is the oscillation frequency, ϕ is the phase, and C_1 (C_2) is the magnitude of the first (second) term. The fitting results are shown in Fig. 3(a) as dotted curves. Figure 3(b) plots the evaluated τ_1 (open circles) and τ_2 (closed circles) as a function of P_{k_1}. Both τ_1 and τ_2 are almost entirely independent of P_{k_1}. Therefore, the effect of excitation-induced dephasing is not the main reason for the shift of the peak $\sqrt{P_{k_2}}$.

Next, we discuss the effect of depolarization of the k_2 field on the excitonic Rabi oscillation. From the analysis curve in Fig. 2(a), we estimated the Rabi frequency Ω using the peak $\sqrt{P_{k_2}}$. The estimated frequency is plotted as a function of $\sqrt{P_{k_1}}$ by the open circles in Fig. 4. The frequency increases with $\sqrt{P_{k_1}}$. However, in this plot, the dipole moment is a variable parameter. Fundamentally, the Rabi frequency, which is evaluated by means of the P_{k_2} dependence of the DFWM intensity, is independent of P_{k_1}. Moreover, the excitonic dipole moment is determined by the sample structure. Therefore, we evaluated the pulse area value for each peak P_{k_2} by using the quasi-dipole moment estimated from the $\sqrt{P_0}$, and the Ω values were estimated from the pulse areas. Ω is plotted as closed circles in Fig. 4. The Ω value decreases with $\sqrt{P_{k_1}}$, owing to the depolarization effect. The external light field $E_{\mathrm{ex}} = E_{\mathrm{L}} + 4\pi NP$ is the light field of P_{k_2}, where E_{L} is the local field inside the thin film, P is the macroscopic polarization, and N is the depolarization tensor.[9] Since the E_{L} term is an effectively parameter in the Rabi oscillation, the decrease in the Rabi frequency is due to the

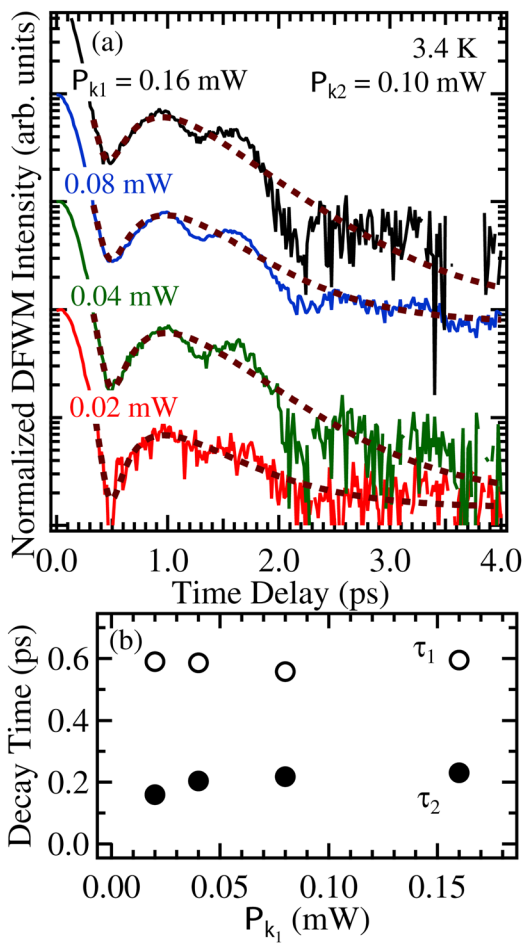

FIG. 3. (Color online) (a) Normalized DFWM signal at various P_{k_1} values shown in Fig. 1(a). Dotted curves indicate the fitting using Eq. (2). (b) Dependence on P_{k_1} of τ_1 (open circles) and τ_2 (closed circles) evaluated by using Eq. (2).

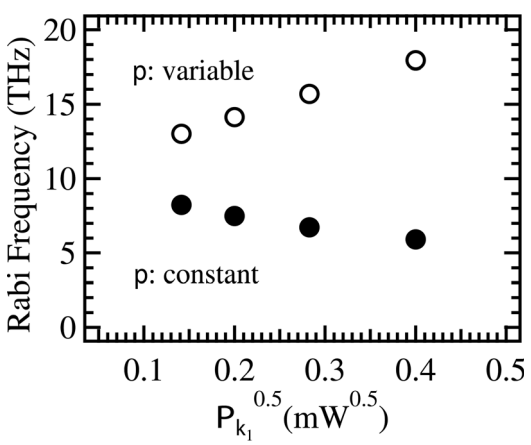

FIG. 4. Rabi frequency estimated from the results of Fig. 2. The values indicated by the open (closed) circles were estimated when p was variable (constant).

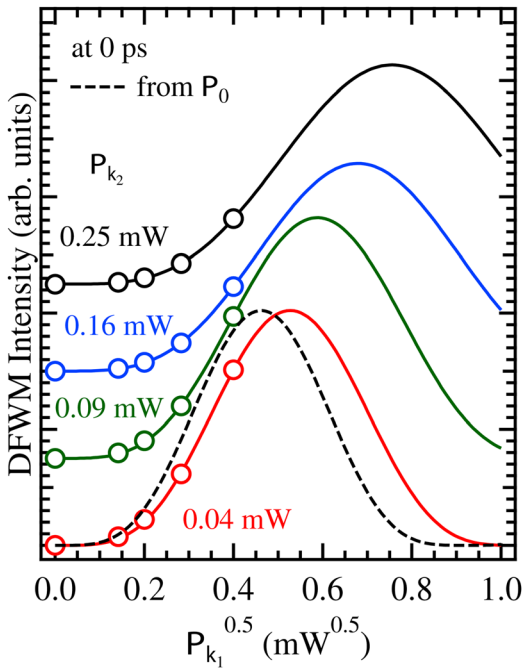

FIG. 5. (Color online) P_{k_1} dependence of I_{DFWM} measured at various P_{k_2} values. Solid curves indicate the analysis curves. The dashed curve indicates the curve calculated by use of P_0.

decrease in E_{L}. Therefore, the shift in the peak intensity in Fig. 2(a) is attributed to the cancellation of the external field by the depolarization factor induced by the k_1 pulse.

B. Pulse area correction

We discuss the correction of the pulse areas by the depolarization due to excitons generated by corresponding pulses. Figure 5 shows a plot of I_{DFWM} as a function of $\sqrt{P_{k_1}}$ measured at various P_{k_2} values. The solid curves indicate the fitting results for the $\sin^4(\Theta_1/2)$ function form. The dotted curve indicates the $\sin^4(\Theta_1/2)$ curve, calculated by use of P_0. The peak $\sqrt{P_{k_1}}$ clearly shifts to a higher power as P_{k_2} increases. To clarify the shift of the peak $\sqrt{P_{k_1}}$ due to the k_2 pulse, the peak $\sqrt{P_{k_1}}$ was evaluated for various P_{k_2} values (Fig. 6). The dotted line indicates the result of least squares fitting to the experimental results. From this fitting, the $\sqrt{P_{k_2}}$ dependence of the peak $\sqrt{P_{k_1}}$ is given by $0.695\sqrt{P_{k_2}} + 0.397$ mW$^{0.5}$. Both the intercept and the gradient values are almost twice those in the case of the $\sqrt{P_{k_1}}$ dependence of peak $\sqrt{P_{k_2}}$, which corresponds to the relation between Θ_1 and Θ_2 in Eq. (1).

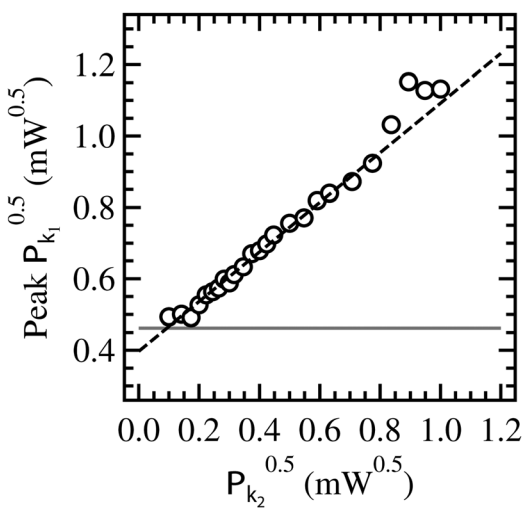

FIG. 6. $P_{k_2}^{0.5}$ dependence of the peak $P_{k_1}^{0.5}$ evaluated in Fig. 5.

The fitting results show that the peaks $\sqrt{P_{k_1}}$ and $\sqrt{P_{k_2}}$ depend on $\sqrt{P_{k_2}}$ and $\sqrt{P_{k_1}}$, respectively. Thus, we simulated the P_{k_1} and P_{k_2} dependence of I_{DFWM} by using an explicit expression of the modified Eq. (1) as follows. Since Θ_2 is equal to $\pi/2$ at $\sqrt{P_{k_2}} = 0.231$ mW$^{0.5}$,

$$I_{\mathrm{DFWM}}(\Theta_2) \propto \sin^2\left(\frac{\pi}{2}\frac{\sqrt{P_{k_2}}}{0.231}\right). \tag{3}$$

To include the peak shift and a term of Θ_1,

$$I_{\mathrm{DFWM}}(\Theta_1,\Theta_2) \propto \sin^2\left(\frac{\pi\sqrt{P_{k_2}}}{0.427\sqrt{P_{k_1}}+0.231}\right) \times \sin^4\left(\frac{\pi\sqrt{P_{k_1}}}{2(0.695\sqrt{P_{k_2}}+0.397)}\right). \tag{4}$$

Moreover, P_{k_1} is changed by increasing with P_{k_2}, so that

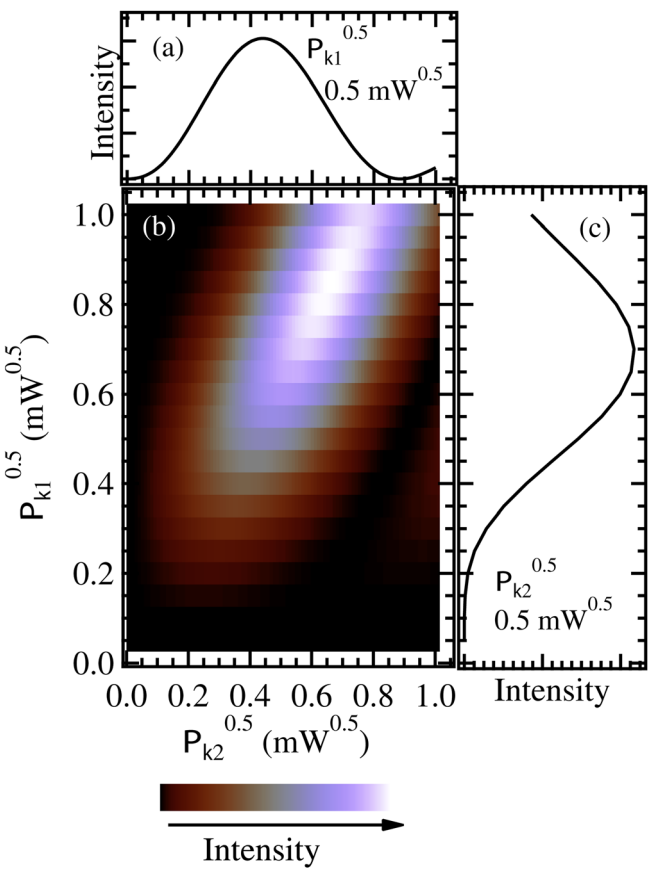

FIG. 7. (Color online) (a) Calculated P_{k_2} dependence of I_{DFWM} at $P_{k_1}^{0.5} = 0.5$ mW$^{0.5}$. (b) Image map of the P_{k_2} dependence of I_{DFWM} at various P_{k_1} values. The brightness is proportional to intensity. (c) Estimated P_{k_1} dependence of I_{DFWM} at $P_{k_2}^{0.5} = 0.5$ mW$^{0.5}$.

$$I_{\mathrm{DFWM}}(\Theta_1,\Theta_2) \propto \sin^2\left(\frac{\pi\sqrt{P_{k_2}}}{0.427\dfrac{\sqrt{P_{k_1}}}{0.695\sqrt{P_{k_2}}+0.397}+0.231}\right) \times \sin^4\left(\frac{\pi\sqrt{P_{k_1}}}{2(0.695\sqrt{P_{k_2}}+0.397)}\right). \quad (5)$$

Figure 7(b) shows an image map of the $\sqrt{P_{k_2}}$ dependence of I_{DFWM} at various $\sqrt{P_{k_1}}$ values with a step of 0.1 $\mathrm{mW}^{0.5}$, where the brightness is proportional to I_{DFWM}. Figures 7(a) and 7(c) show the $\sqrt{P_{k_2}}$ and $\sqrt{P_{k_1}}$ dependence at $\sqrt{P_{k_1}}$ and $\sqrt{P_{k_2}}$ of 0.5 $\mathrm{mW}^{0.5}$, respectively, for reference. The simulation results clearly demonstrate the shift of I_{DFWM} to higher power sides. However, the simulated profiles in Figs. 7(a) and 7(c) do not show the asymmetric profile on the higher power side. Moreover, the simulated I_{DFWM} drops to zero. In other words, our simulation indicates that the shift of I_{DFWM} originates from depolarization; however, the asymmetric profile and I_{DFWM} always being nonzero cannot be explained by only the depolarization effect.

IV. CONCLUSION

We investigated the effects of depolarization on the ultrafast optical control of exciton polarization confined in GaAs thin films by use of Rabi oscillation. In the DFWM signal along the $2k_1 - k_2$ direction, the Rabi frequency, evaluated from the k_2-power dependence, decreased with P_{k_1}. This decrease in the Rabi frequency originated from the cancellation of the k_2 light field due to depolarization induced by the excitons generated by the k_1 pulses. The analysis of the Rabi frequency clarifies the intrinsic excitonic "quasi" dipole moment and the depolarization factor. This work suggests an approach to realizing coherent optical control of excitons confined in the solid state. Straightforwardly, the suppression of the depolarization factor can lead to low-power operation.

ACKNOWLEDGMENTS

This work was partially supported by Grants-in-Aid for Scientific Research from the Ministry of Education, Culture, Sports, Science, and Technology (MEXT) of Japan and for Scientific Research on Innovative Areas "Optical Science of Dynamically Correlated Electrons" from MEXT of Japan and by Grant-in-Aid from the Research Foundation for Opto-Science and Technology of Japan.

[1] J. M. Hvam, Ultrafast Photonics, edited by A. Miller, D. T. Reid, and D. M. Finlayson (Institute of Physics, London, 2004), p. 265.
[2] O. Wada, New J. Phys. **6**, 183 (2004).
[3] O. Kojima, T. Isu, J. Ishi-Hayase, A. Kanno, R. Katouf, M. Sasaki, and M. Tsuchiya, Phys. Status Solidi C **5**, 2858 (2008).
[4] S. T. Cundiff, A. Knorr, J. Feldmann, S. W. Koch, and E. O. Göbel, Phys. Rev. Lett. **73**, 1178 (1994).
[5] B. Patton, U. Woggon, and W. Langbein, Phys. Rev. Lett. **95**, 266401 (2005).
[6] A. J. Ramsay, A. V. Gopal, E. M. Gauger, A. Nazir, B. W. Lovett, A. M. Fox, and M. S. Skolnick, Phys. Rev. Lett. **104**, 017402 (2010).
[7] M. Kujiraoka, J. Ishi-Hayase, K. Akahane, N. Yamamoto, K. Ema, and M. Sasaki, Phys. Status Solidi A **206**, 952 (2009).
[8] M. Kujiraoka, J. Ishi-Hayase, K. Akahane, N. Yamamoto, K. Ema, and M. Sasaki, Appl. Phys. Express **3**, 092801 (2010).
[9] G. Y. Slepyan, S. A. Maksimenko, A. Hoffmann, and D. Bimberg, Phys. Rev. A **66**, 063804 (2002).
[10] G. Y. Slepyan, A. Magyarov, S. A. Maksimenko, A. Hoffmann, and D. Bimberg, Phys. Rev. B **70**, 045320 (2004).
[11] E. Paspalakis, A. Kalini, and F. Terzis, Phys. Rev. B **73**, 073305 (2006).
[12] O. Kojima, T. Isu, J. Ishi-Hayase, A. Kanno, R. Katouf, M. Sasaki, and M. Tsuchiya, J. Phys. Soc. Jpn. **77**, 044701 (2008).
[13] O. Kojima, A. Miyagawa, T. Kita, O. Wada, and T. Isu, Appl. Phys. Express **1**, 112401 (2008).
[14] O. Kojima and T. Isu, *High-Power and Femtosecond Lasers: Properties, Materials and Applications*, edited by P.-H. Barret and M. Palmer (Nova Science, New York, 2009), p. 441.
[15] O. Kojima, S. Watanabe, T. Kita, O. Wada, and T. Isu, Phys. Status Solid C, **8**, 378 (2011).
[16] O. Kojima, S. Watanabe, T. Kita, O. Wada, and T. Isu, J. Phys. Soc. Jpn. **80**, 034704 (2011).
[17] H. Ishihara, K. Cho, K. Akiyama, N. Tomita, Y. Nomura, and T. Isu, Phys. Rev. Lett. **89**, 17402 (2002).
[18] I. Abram, Phys. Rev. B **40**, 5460 (1989).
[19] In this sample, the response by the second confined heavy-hole exciton is dominant. In addition, the long-wavelength approximation is not applicable due to the thickness. Therefore, the term "dipole moment" is not accurate, and hence, we use the term "quasi-dipole moment".
[20] K. Leo, E. O. Göbel, T. C. Damen, J. Shah, S. Schmitt-Rink, W. Schäfer, J. F. Müller, K. Köhler, and P. Ganser, Phys. Rev. B **44**, 5726 (1991).